



Soil pollution and toxicity in an area affected by emissions from a bauxite processing plant and a power plant in Gardanne (southern France)

Rahime Oral^a, Giovanni Pagano^{b,c,*}, Antonietta Siciliano^b, Maria Toscanesi^b, Maria Gravina^b, Aldo Di Nunzio^b, Anna Palumbo^c, Philippe J. Thomas^d, Franca Tommasi^e, Petra Buric^f, Daniel M. Lyons^g, Marco Guida^b, Marco Trifuoggi^b

^a Ege University, Faculty of Fisheries, TR-35100 Bornova, İzmir, Turkey

^b Federico II Naples University, I-80126 Naples, Italy

^c Stazione Zoologica Anton Dohrn, I-80121 Naples, Italy

^d Environment and Climate Change Canada, Science & Technology Branch, National Wildlife Research Center – Carleton University, Ottawa, Ontario, Canada K1A 0H3

^e Aldo Moro Bari University, Department of Plant Biology, I-70124 Bari, Italy

^f Juraj Dobrila University of Pula, HR-52100 Pula, Croatia

^g Center for Marine Research, Ruđer Bošković Institute, HR-52210 Rovinj, Croatia

ARTICLE INFO

Keywords:

Soil pollution
Soil toxicity
Bauxite processing
Power plant
Sea urchins
C. elegans

ABSTRACT

Soil pollution and toxicity have been investigated in the Gardanne area (southern France) at a range of sites around a recognized pollution source, a bauxite processing plant (BPP), and a power plant (PP). Soil samples were submitted to inorganic and organic analyses and tested for toxicity in two invertebrate models. Inorganic analysis was based on determining elemental concentrations by ICP-MS, encompassing a total of 26 elements including 13 rare earth elements (REEs), of the soil samples and their leachates after 24 or 48 h in seawater. Organic analyses were performed by measuring the sums of 16 polycyclic aromatic hydrocarbons (PAHs) and of total hydrocarbons (C-10 to C-40). Bioassays were carried out on the early life stages of three sea urchin species (*Arbacia lixula*, *Paracentrotus lividus* and *Sphaerechinus granularis*), and on a nematode (*Caenorhabditis elegans*). Sea urchin bioassays were evaluated by the effects of soil samples (0.1–0.5% dry wt/vol) on developing embryos and on sperm, and scored as: a) % developmental defects, b) inhibition of sperm fertilization success and offspring damage, and c) frequencies of mitotic aberrations. *C. elegans* 24 h-mortality assay showed significant toxicity associated with soil samples. The effects of soil samples showed heightened toxicity at two groups of sites, close to the BPP main entrance and around the PP, which was consistent with the highest concentrations found for metals and PAHs, respectively. Total hydrocarbon concentrations displayed high concentrations both close to BPP main entrance and to the PP. Further studies of the health effects of such materials in Gardanne are warranted.

1. Introduction

Bauxite manufacturing by the Bayer process in alumina production is associated with a by-product, bauxite residue (BR), traditionally termed “red mud” (Xue et al., 2016; Xu et al., 2018). In turn, BR has raised environmental concern in areas affected by plant effluents as related to its recognized toxicity since early studies (Trief et al., 1995; His et al., 1996; Dauvin, 2010; Howe et al., 2011; Klebercz et al., 2012). Beyond BR as a complex mixture, its main elemental components, aluminum and iron, have been investigated for their adverse effects in human and environmental health (Pagano et al., 1996; Mišić et al., 2014; reviewed by Willhite et al., 2014). Thus BR, as a complex mixture

arising from alumina production is not confined to fluid “red mud” or to marine sediments (due to offshore BR disposal), but should also be regarded as a pollutant which may additionally affect the terrestrial environment near bauxite processing plants (BPPs). Recent reports have focused on the impacts of BR disposal areas, providing evidence for persistent alterations of soil and freshwaters composition near BPPs (Ren et al., 2018; Olszewska et al., 2016; Higgins et al., 2017). Management steps to suppress dusting from BR-polluted areas using phytostabilization has gained much interest (e.g. Courtney et al., 2011; Higgins et al., 2017) but the possibility of fugitive dusting from operational or legacy sites remains.

We reported previously on soil pollution and toxicity in Gardanne

* Corresponding author at: Federico II Naples University, I-80126 Naples, Italy.
E-mail address: gbpagano@tin.it (G. Pagano).

and at other two sites close to BPPs (in Italy and in Turkey) (Pagano et al., 2002a, 2002b). Those studies left some open questions related to possible changes in the management of pollutant release from the plants. Moreover, those previous studies were confined following metal leaching from soil inorganic analysis (using a scarcely sensitive method, ICP-OES), and sample processing before analysis was only performed by seawater suspension, without a parallel procedure by acid dissolution of soil samples. As a major limitation, the previous study failed to provide any data on organic soil pollution, possibly related to emissions from the nearby power plant (PP). In turn, the recent literature has pointed to fly ash release from PPs, both including inorganics (Raja et al., 2015; Haberl et al., 2018) and several organic classes, such as polycyclic aromatic hydrocarbons (PAHs) (Twardowska and Schramm, 2000; Ruwei et al., 2013), combustion-derived nanoparticles (CDNP), and *de novo* formation of polychlorinated dibenzo-p-dioxins and dibenzofurans (PCDDs and PCDFs) (Wikström et al., 2003; Freire et al., 2015). Thus, the combined presence in Gardanne of a BPP and of a fluid bed coal- (then biomass-) combusting PP warranted undertaking a new investigation encompassing both soil inorganic analysis (by means of the more sensitive ICP-MS method) and organic analysis (PAHs and total hydrocarbons, C-10 to C-40).

This new series of determinations was aimed at determining temporal changes, if any, of metal and organic pollutant concentrations on a topographic basis around the BPP. Thereafter, by evaluating soil samples in the wider Gardanne industrial area, higher levels of soil pollution were also detected near the PP.

A new hypothesis, and tested in the current study, was that the occurrence of rare earth elements (REEs) in bauxite ore and in bauxite processing residues (Karadağ et al., 2009; Pagano et al., 2015) could be tracked and used as a proxy for soil contamination as a consequence of the bauxite refining process.

Thus, metal analysis on soil samples included REEs, also in view of their possible (phyto)extraction from bauxite ore or bauxite by-products (Haberl et al., 2018; Higgins et al., 2017; Jacinto et al., 2018).

In parallel with these analyses, toxicity testing was conducted on soil samples by means of bioassays on a marine and a terrestrial bioassay model, namely the early life stages of three sea urchin species (*Arbacia lixula*, *Paracentrotus lividus* and *Sphaerechinus granularis*), and of a nematode (*Caenorhabditis elegans*) mortality bioassay.

Overall, the analytical data were consistent with the toxicity findings both in sea urchin and nematode bioassays.

2. Methods

2.1. Study area and sampling sites

As shown in Fig. 1, the Gardanne (43°45'25.98" N, 5°47'17.36" E) industrial area investigated herein includes a BPP and nearby PP, which are located close to the residential neighborhoods of the town.

2.2. Soil sample collection and processing

A total of 14 topsoil samples were collected from road or street edges by a shovel in amounts of approximately 100 g, after removing any gross stony or plant materials, and carried to the lab in polystyrene 150-ml beakers. The samples were sieved in 2-mm mesh steel nets and then ground to a fine powder in a ceramic pestle. Subsequently, samples to be analyzed and tested in bioassays were dried at 60 °C.

2.3. Elemental analysis

Soil samples were analyzed for inorganic content, for 13 analyzed elements and 13 REEs. Soil samples were subjected to microwave-assisted acid oxidative digestion using a mixture of acids at high temperature (up to 180 °C) and pressure (Mars – CEM, Italy). For bringing metals into solution, the US EPA 3051A (2007) method was used while

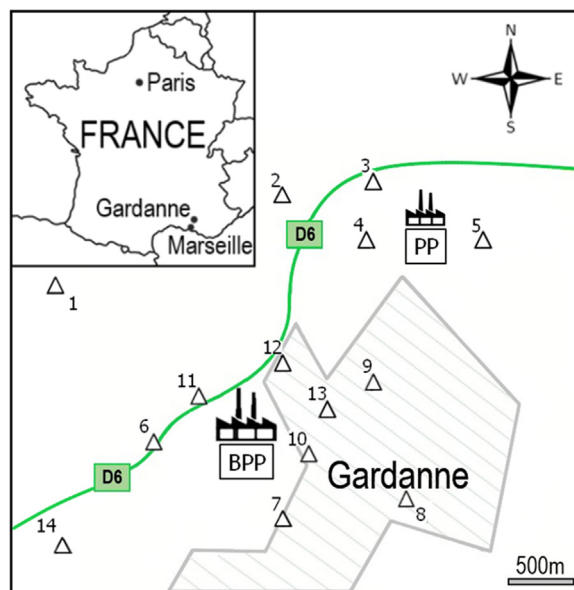


Fig. 1. Map of Gardanne (40°26'46" N 79°58'56" W), southern France, and of soil sampling points. Abbreviations: BPP – Bauxite Processing Plant; PP – Power Plant.

acid digestion was carried out using an internal method that involved two steps;

nitric and hydrofluoric acid were first used followed by the addition of boric acid.

Quantitative determination was carried out with the method ISO 17294-2:2016 by means of ICP-MS analysis (inductively coupled plasma mass spectrometry) (Aurora M90 Bruker, USA). The limit of detection (LOD) and limit of quantification (LOQ) were calculated using the method of blank variability for each investigated metal.

Based on the recognized association of BR with increased REE concentrations (Karadağ et al., 2009; Pagano et al., 2015), soil samples were analyzed for their REE content (13 elements, from Y to Yb).

In order to evaluate potential metal release from soil samples that may occur during the bioassays, soil samples were suspended and stirred either in filtered seawater and the solutions analyzed for dissolved metal content after 24 and 48 h. Each analysis was run in triplicate; given the overlapping results following 24- and 48 h, the respective results were merged as six-replicate means \pm SEM.

2.4. PAH and total organic analysis

Soil samples were analyzed for PAH and total hydrocarbon (C10–C40) contents. The analyzed PAH homologs were: Acenaphthylene; Acenaphthylene; Anthracene; Benzo(a)anthracene; Benzo(b)fluoranthene; Benzo(k)fluoranthene; Benzo(g,h,i)perylene; Benzo(a)pyrene; Crysene; Dibenzo(a,h)anthracene; Fluorene; Fluoranthene; Indenopyrene; Naphthalene; Phenanthrene and Pyrene. The dry soil samples were extracted with a mixture acetone/n-hexane 1:1 vol/vol with sonication for 3 h by ultrasonic disruptor. The extract was purified with florisil, analyzed by gas chromatography coupled with a mass spectrometer (Shimadzu 2010 Plus and MS-TQ8030-Shimadzu, Japan) for PAHs while total hydrocarbons were analyzed by gas chromatography with flame ionization detector (FID) (Agilent 6890, USA). Triplicate determinations were carried out and data were reported as mean \pm SEM.

For the qualitative and quantitative analysis the external calibration method was used (APHA, 1998). The limit of detection (LOD) and limit of quantification (LOQ) were calculated using the range method of prediction to 95% of linear regression for each investigated PAH. The calculated average values of LOD and LOQ were 0.03 and 0.1 $\mu\text{g/g}$,

respectively.

The acetone/hexane extract for total hydrocarbons (C10–C40) analysis was purified with florisil, and analyzed by gas chromatography with Flame Ionization detector (FID) (Agilent 6890, USA).

Data accuracy was checked by reference certified materials [BCR-CRM 535 (PAH), BCR-CRM 667 and 277R]. Performance was verified through participation in inter-laboratory intercalibration.

2.5. Sea urchin assays

Sea urchins from three species (*Paracentrotus lividus*, *Arbacia lixula* and *Sphaerechinus granularis*) were collected along the Çeşme coast, Turkey (38°32'43" N, 26°30'32" E), the Bay of Naples, Italy (40°51'11.86" N, 14°18'20" E), and the Rovinj coast, Croatia (45°04'47" N, 13°38'24" E), respectively. Gametes were obtained, and embryo cultures were prepared as described previously (Pagano et al., 2001, 2017). Controls were conducted as untreated negative controls in natural filtered seawater (FSW) from offshore, salinity 3.5‰, pH 8. No "pristine" soil control was utilized due to the expected – and verified – differences in soil toxicity that allowed for distinctions within the sample sets according to their topographic distribution.

In embryotoxicity tests, dry soil aliquots (0.1% wt/vol) were placed at the bottom of each well of standard culture plates [Falcon™ Tissue Culture Plates (6 wells, 10 ml/well, code # 353046)], and then suspended in 9 ml FSW. Thereafter, 1 ml of zygotes (~200–300 embryos, 10 min post-fertilization (p-f)) was added to soil suspensions and incubated at 18 °C in the dark for 72 h. The embryos were thus exposed throughout development up to the pluteus larval stage.

Cytogenetic analysis was carried out on soil sample-exposed embryos (fixed 5 h p-f) and three endpoints were evaluated in the mitotic activity of cleaving embryos, i.e.: a) mean number of mitoses per embryo; b) % interphase embryos, lacking active mitoses, and c) % embryos with ≥ 1 mitotic aberrations. Thus, both mitotic inhibition (a, b) and aberration frequency (c) could be evaluated.

Sperm bioassays were performed on *S. granularis* sperm suspensions: a 100-μl sperm pellet was suspended in 10 ml of stirred soil sample suspensions (0.5% wt/vol). After 10 min, a 100-μl aliquot of sperm-containing supernatant was used to inseminate untreated egg suspensions. Thus, the ensuing offspring embryos developed without contact with soil samples.

Changes in fertilization rate (FR = % fertilized eggs) of exposed sperm were determined by scoring the percent of fertilized eggs in live cleaving embryos (1–3 h p-f). Thereafter, 72 h p-f, the offspring derived from exposed sperm was scored for developmental defects as in the embryotoxicity bioassays.

Each bioassay was run in six replicates. Larvae were immobilized by 10⁻⁴ M chromium sulfate 5 min prior to observation (Pagano et al., 1983), and the first 100 plutei in each replicate culture 72 h p-f were scored. The following outcomes regarding embryogenesis abnormalities were scored: i) pathologic (P1), malformed plutei; ii) pathologic embryos (P2), arrested at pre-larval stages, and iii) dead (D) embryos. The total percentages of P1 + P2 + D were scored blind by trained readers, each of whom evaluated a complete set of cultures.

2.6. *Caenorhabditis elegans* bioassays

The nematode bioassay was carried out, with a few modifications, according to the ASTM E2172 – 01 Standard Method (2014) using the nematode *Caenorhabditis elegans* wild-type strain N2 variant Bristol, maintained on NGM (nematode growth media) plates seeded with *Escherichia coli* (strain OP50-Uracil deficient) and stored at 20 °C. The tests were performed using age-synchronous adult nematodes and achieved by lysis of the gravid nematodes with a bleaching mixture (10 g/l NaOH, 10.5 g/l NaOCl) followed by centrifuge washing with M9 mineral medium (2.2 mM KH₂PO₄, 4.2 mM Na₂HPO₄, 85.6 mM NaCl, 1 mM MgSO₄) and allowed to rest overnight in NGM agar plates.

Soil samples (2.33 g) were hydrated to 35–45% of their dry weight with K-medium in centrifuge tubes. Ten worms were transferred to each test tube and exposed for 24 h at 20 °C to the soil samples. All treatments were done in four replicates, without feeding the worms. Nematodes were extracted from the soil samples by centrifugation (at 2000 rpm for 2 min) using a silica gel with a specific density of 1.13 g/ml (Ludox™ 50, Sigma-Aldrich, St. Louis, MO, USA). After centrifugation, the supernatant of each sample was placed in 100-mm glass Petri dishes and washed with Keller K-medium. The extracted individuals were then counted under a microscope (40× magnification) with mortality as the measured endpoint, and test acceptability requiring 80% recovery and 90% control survival.

2.7. Statistical analysis

Results of bioassays are given as the mean ± standard error. Differences between samples and the control group were determined by a two-tailed Student's *t*-test. The significance of differences among groups was evaluated by one-way analysis of variance (ANOVA) and further statistical post-hoc comparisons with Tukey's multiple comparison test. The variables that were unsuitable for parametric statistics were evaluated with nonparametric tests including the χ^2 test and Mann–Whitney *U* test. Differences were considered significant when *p* < 0.05.

3. Results

3.1. Inorganic analysis

Following acid oxidative digestion, metal concentrations were measured in soil samples. Iron and aluminum displayed the highest concentrations (> 1000 mg/kg) in samples from sites 1, 8, 9 and 13. Lower concentrations were found for Mn with a range of 18–34 mg/kg noted among the sites. The sum of REE concentrations showed the third highest concentration at all the sites, with the highest concentrations of 20–25 mg/kg noted at sites 1, 8 and 9. The other measured elements (Zn, Pb, V, Cr, Ni, Cu and B) showed far lower concentrations (1–6 mg/kg), except for Pb and Zn at site 5 (14 and 29 mg/kg). The lowest measured concentrations were found for Co, Sn, As, and Sb (< 1 mg/kg) (data not shown).

Analysis of metal leaching from soil samples in seawater over 24 and 48 h showed that aluminum and iron had by far the highest concentrations with values > 200 μg/l noted. As shown in Fig. 2, Al concentrations were highest at the distant site 1, at sites 2 and 3 (close to the PP), and at sites 9 and 11 (eastern side of the BPP). Leaching of Fe showed the highest concentrations from soil samples collected from sites 1, 2 and 3 and another concentration peak at site 9.

Other elements (B, V, Zn and As) leached from the soils were present at concentrations of ≤ 50 μg/l, with significantly highest concentrations found for samples from sites 10 and 12 (close to the BPP) and very low concentrations in samples from sites 1 to 4. Thus, except for Al and Fe, leached metals (B, V, Zn and As) showed a concentration gradient with significantly highest values noted for sites near the BPP and gradually diminishing with increasing distance from the BPP (i.e. intermediate sites 5–8, to distant sites 1–4). The sum of leached REE concentrations were found evenly distributed across sampling sites and in the order of < 10 μg/l (data not shown).

3.2. Organic analysis

The sum of PAH concentrations showed highest values at sites 2 and 7 (10–15 mg/kg) (Fig. 3A), without displaying excess PAH concentrations either close to the BPP or the PP. Unlike PAHs, total hydrocarbons (C10–C40) showed significantly excess concentrations in the area nearby the entrance of the BPP (sites 10 and 12), as shown in Fig. 3B.

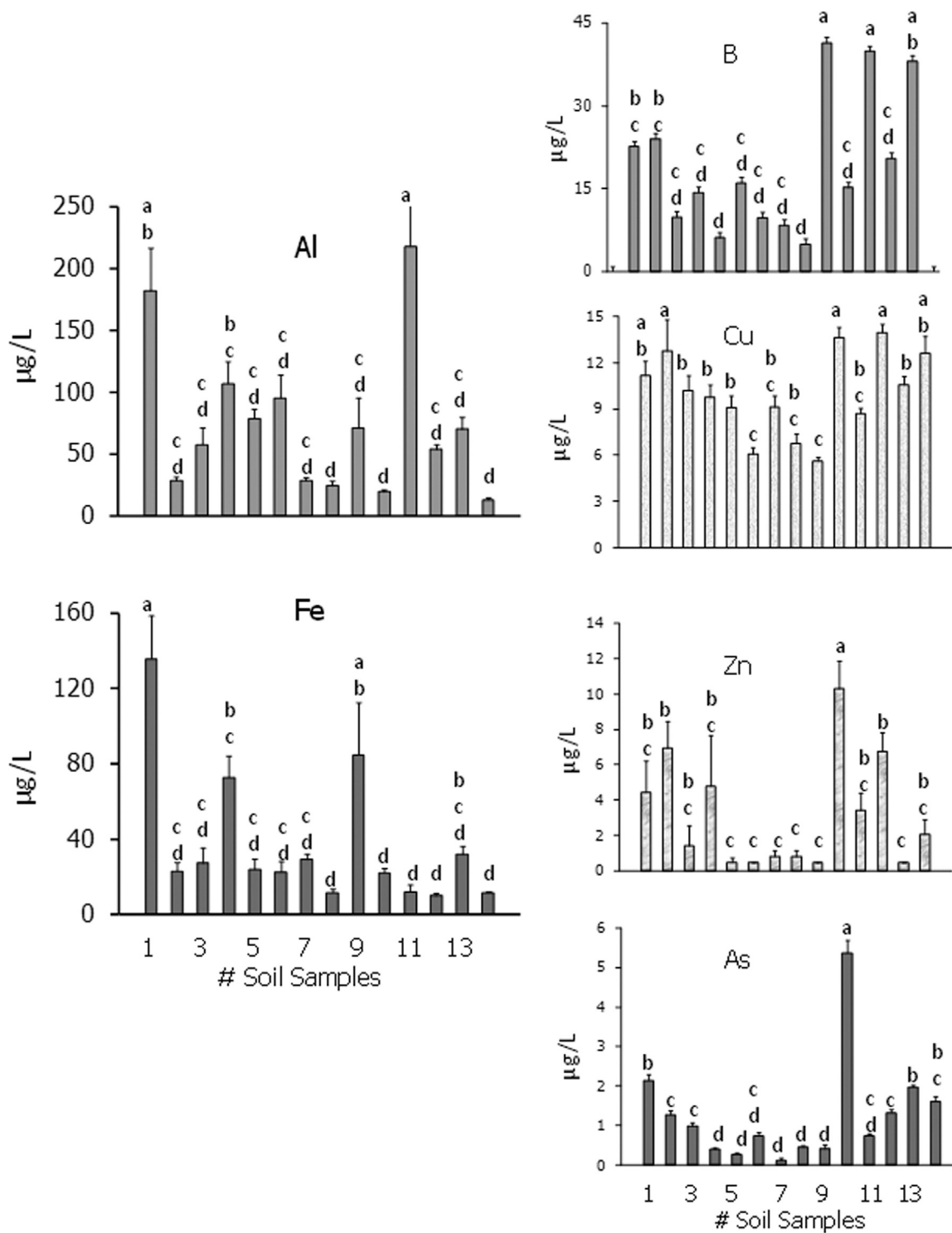


Fig. 2. Measured Al and Fe concentrations in soil samples, and measured B, V, Zn and As concentrations in soil samples following 24- to 48-h soil seawater suspension. Six-replicate determinations; data (µg/l) are expressed as means ± SEM. Data with different letters (a–d) are significantly different (p < 0.05).

3.3. Sea urchin bioassays

By rearing sea urchin embryos of the three tested species, *A. lixula* larvae displayed a significant excess of developmental defects (DD) following exposure to 0.1% soil samples from sites 5, 11 and 12 (Fig. 4). *P. lividus* larvae were found most affected by soil samples from sites 3, 5, and from sites 10–12 and 14, whereas *S. granularis* larvae showed excess DD following exposure to soil from sites 3, and 10–12. Overall, excess DD were exerted by soil samples both from sites close to PP (3

and 5) and close to the BPP (10–12).

Cytogenetic analysis of 0.1% soil-exposed embryos failed to show any site-related inhibition of mitotic activity, measured as mitoses per embryo or as % interphase embryos (data not shown). As for the induction of mitotic aberrations, measured as % embryos with ≥ 1 mitotic aberrations, site-related effects were observed in embryos of the three species, as shown in Fig. 5. Soil exposure of *A. lixula* embryos resulted in a significant excess of mitotic aberrations for sites 5–6 and 10–12. *P. lividus* embryos underwent significantly increased mitotic

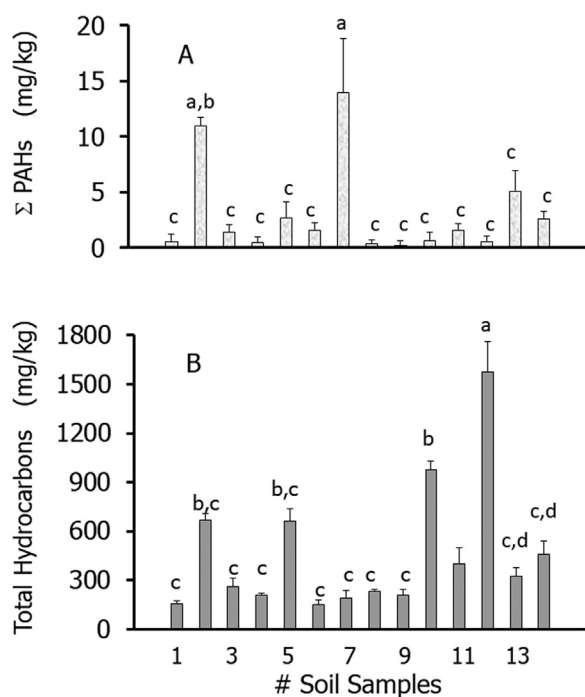


Fig. 3. A. Concentrations of PAH sums in soil samples following organic extraction. Triplicate determinations; data ($\mu\text{g/l}$) are expressed as means \pm SEM. Data with different letters (a–c) are significantly different ($p < 0.05$). B. Concentrations of total hydrocarbons (C10–C40) in soil samples following organic extraction. LOD and LOQ were 1.7 and 5.1 mg/kg.

aberrations when exposed to soil samples from sites 2–5 and 11–12, while *S. granularis* embryos displayed the highest rates of mitotic aberrations when exposed to soil samples from sites 5, 8–10, and 12. Thus, similar to the induction of larval developmental defects, mitotic aberrations were significantly increased for samples from the areas near the PP (sites 3–5) and near the BPP (sites 10–12).

When *S. granularis* sperm were exposed to the soil sample suspensions, a significant inhibition of fertilization rate (FR) was observed for sites 3, 5 and 11, whereas no significant FR inhibition was noted from soil samples from the other sites. Concurrent with FR decrease, the offspring of soil-exposed sperm also underwent significantly increased developmental defects for sites 3, 5, and 11, as shown in Fig. 6.

3.4. Nematode bioassays

By exposing *C. elegans* to soil samples ($\cong 30\%$ wt/vol), a significantly increased 24-h mortality was observed for all soil samples, though the highest mortality frequencies were detected following exposures to soil samples from sites 5 and 11 (Fig. 7).

4. Discussion

The concentrations of a range of metals (Al, Fe, B, V, Zn and As) and analyses of total hydrocarbons (C10 to C40) indicated similar patterns in the Gardanne area close to the BPP (sites 9–12) and surrounding the PP sites 2–5. These findings were consistent with the literature where PP emissions are associated with multiple organic-based types of pollution (Twardowska and Schramm, 2000; Ruwei et al., 2013; Kruse et al., 2014; Freire et al., 2015; Raja et al., 2015), though the impact of the metal component in fly ash of waste-to-energy plants has also been investigated (Haberl et al., 2018). The established roles of polychlorinated biphenyls, polychlorinated dibenzo-p-dioxins and polychlorinated dibenzofurans in PP-polluted soils (Twardowska and Schramm, 2000; Kruse et al., 2014) was not investigated in the present study although it may be speculated that the Gardanne PP emissions

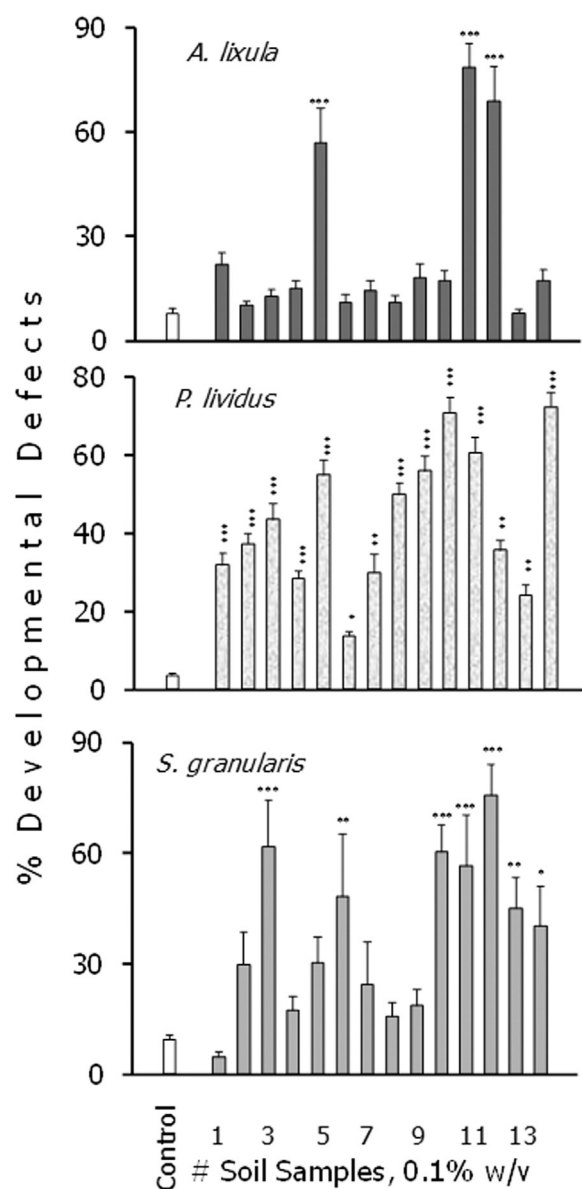


Fig. 4. Induction of developmental defects following exposure (72 h post-fertilization) of embryos/larvae of three sea urchin species (*A. lixula*, *P. lividus* and *S. granularis*). Significance: * $p < 0.05$; ** $p < 0.01$; *** $p < 0.001$. Same as in Figs. 5–7.

might also be a source of such pollutants thereby warranting *ad hoc* investigations.

With respect to the finding of decreasing soil metal content with distance from point sources of pollutants, an exception was noted for site 1, which was located far from the BPP and PP, with high Al, Fe and B concentrations measured. This anomaly confirms previous data (Pagano et al., 2002a) and may be related to atmospheric deposition of BPP-derived dust based on prevailing weather patterns. Thus a further question arises on what the possible impacts of such deposition on surrounding agricultural land may be, taking into consideration the soils' natural composition.

Another unexpected observation was found in the soil concentrations of total hydrocarbons that displayed two peaks, close to the PP (sites 2 and 5) and close to the BPP (sites 10 and 12). It should be noted that sites 10 and 12 are located near to the entrance to the BPP and are affected by intensive truck traffic involved in bauxite transportation, hence the likely source of high concentrations of aliphatic hydrocarbons, and as reported previously in heavy traffic areas (Azimi et al.,

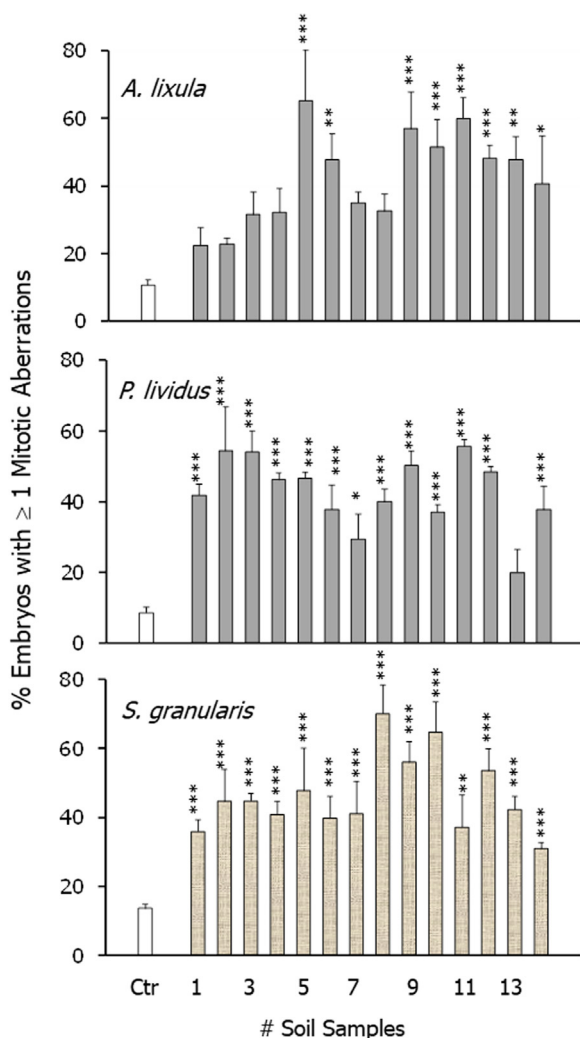


Fig. 5. Percent embryos displaying ≥ 1 mitotic aberrations in embryos from three sea urchin species (*A. lixula*, *P. lividus* and *S. granularis*) exposed to 0.1% soil samples.

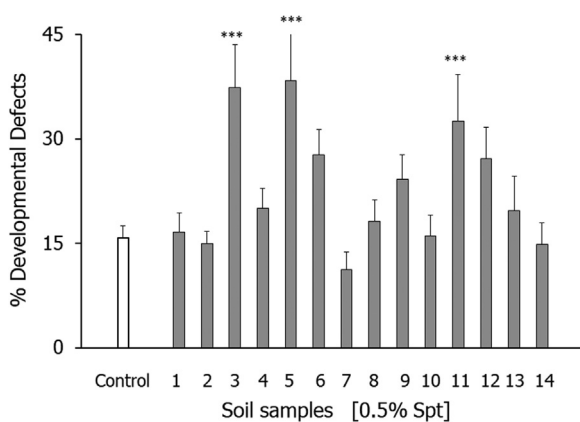


Fig. 6. Offspring damage (% developmental defects) following *S. granularis* 10-min sperm exposure to 0.5% soil samples.

2005; Gentner et al., 2012).

The sea urchin bioassays provided evidence for a spatial distribution of soil toxicity, showing some variability between the three tested sea urchin species and among the different endpoints, namely embryotoxicity, cytogenetic damage, fertilization inhibition, and offspring damage following sperm exposure to soil suspension.

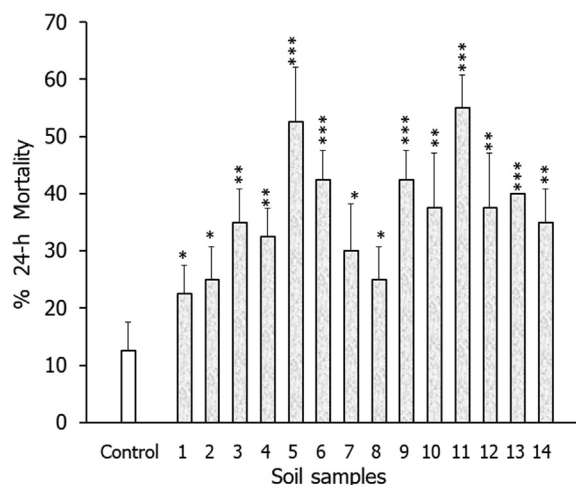


Fig. 7. 24-h % Mortality of *Caenorhabditis elegans* exposed to $\cong 40\%$ (dry wt/vol) of soil samples.

Altogether, the results showed two main peaks of soil toxicity, namely at sites 2–5 and at sites 10–12, consistent with the previously mentioned areas close to the PP and near the entrance of the BPP.

The consistency of the results obtained in sea urchin bioassays with the findings of metals analysis confirms the broad applicability of this bioassay model. Though this is based on a marine organism, its wide range of endpoints made this bioassay useful for broad-ranging complex mixtures, including terrestrial substrates such as soil or land-based pollutants (reviewed in Pagano et al., 2017) and is the focus of a growing body of literature on the use of sea urchins and of other marine biota in toxicity testing of terrestrial and freshwater mixtures (reviewed in Chen and Liu, 2006; Kobayashi and Okamura, 2005; Pagano et al., 2001; Sánchez-Marín and Beiras, 2012; Vazquez, 2013).

This, and the already high concentrations of pollutants have generally led to significant soil toxicity in *C. elegans* ($p < 0.05$ – 0.01), with even greater significance for the 24-h mortality endpoint for sites 5 and 11 ($p < 0.001$).

Altogether, both the sea urchin and the nematode bioassay data corroborated the analytical evidence for increased pollution in two distinct areas, close to the BPP and to the PP.

Whether, and if so to what extent, the analytical and bioassay data may raise some concern in terms of environmental and human health, is a sensitive question warranting further investigations in the Gardanne residential and agricultural areas.

References

APHA, 1998. Standard Methods for the examination of water and waste water American Public Health Association, pp. 874.

ASTM E2172 - 01, 2014. Standard Guide for Conducting Laboratory Soil Toxicity Tests with the Nematode *Caenorhabditis elegans*. ASTM.

Azimi, S., Rocher, V., Muller, M., Moilleron, R., Thevenot, D.R., 2005. Sources, distribution and variability of hydrocarbons and metals in atmospheric deposition in an urban area (Paris, France). *Sci. Total Environ.* 337, 223–239.

Chen, C.M., Liu, M.C., 2006. Ecological risk assessment on a cadmium contaminated soil landfill – a preliminary evaluation based on toxicity tests on local species and site-specific information. *Sci. Total Environ.* 359, 120–129.

Courtney, R., Keith, A.M., Harrington, T., 2011. Nematode assemblages in bauxite residue with different restoration histories. *Restor. Ecol.* 19, 758–764.

Dauvin, J.C., 2010. Towards an impact assessment of bauxite red mud waste on the knowledge of the structure and functions of bathyal ecosystems: the example of the Cassidaigne canyon (north-western Mediterranean Sea). *Mar. Pollut. Bull.* 60, 197–206.

Freire, M., Lopes, H., Tarelho, L.A., 2015. Critical aspects of biomass ashes utilization in soils: composition, leachability, PAH and PCDD/F. *Waste Manag.* 46, 304–315.

Gentner, D.R., Isaacman, G., Worton, D.R., Chan, A.W., Dallmann, T.R., Davis, L., Liu, S., Day, D.A., Russell, L.M., Wilson, K.R., Weber, R., Guha, A., Harley, R.A., Goldstein, A.H., 2012. Elucidating secondary organic aerosol from diesel and gasoline vehicles through detailed characterization of organic carbon emissions. *Proc. Natl. Acad. Sci. USA* 109, 18318–18323.

- Haberl, J., Koralewska, R., Schlumberger, S., Schuster, M., 2018. Quantification of main and trace metal components in the fly ash of waste-to-energy plants located in Germany and Switzerland: an overview and comparison of concentration fluctuations within and between several plants with particular focus on valuable metals. *Waste Manag.* 75, 361–371.
- Higgins, D., Curtin, T., Courtney, R., 2017. Effectiveness of a constructed wetland for treating alkaline bauxite residue leachate: a 1-year field study. *Environ. Sci. Pollut. Res.* 24, 8516–8524.
- His, E., Beiras, R., Seaman, M.N., Pagano, G., Trieff, N.M., 1996. Sublethal and lethal toxicity of aluminum industry effluents to early developmental stages of the *Crassostrea gigas* oyster. *Arch. Environ. Contam. Toxicol.* 30, 335–339.
- Howe, P.L., Clark, M.W., Reichelt-Brushett, A., Johnston, M., 2011. Toxicity of raw and neutralized bauxite refinery residue liquors to the freshwater cladoceran *Ceriodaphnia dubia* and the marine amphipod *Paracalliope australis*. *Environ. Toxicol. Chem.* 30, 2817–2824.
- ISO 17294-2:2016. Water quality – Application of inductively coupled plasma mass spectrometry (ICP-MS) Determination of selected elements including uranium isotopes.
- Jacinto, J., Henriques, B., Duarte, A.C., Vale, C., Pereira, E., 2018. Removal and recovery of Critical Rare Elements from contaminated waters by living *Gracilaria gracilis*. *J. Hazard. Mater.* 344, 531–538.
- Karadağ, M.M., Küpeli, Ş., Arık, F., Ayhan, A., Zedef, V., Döyem, A., 2009. Rare earth element (REE) geochemistry and genetic implications of the Mortaş-bauxite deposit (Seydişehir/Konya – southern Turkey). *Chem. Erde* 69, 143–159.
- Klebercz, O., Mayes, W.M., Ánton, A.D., Feigl, V., Jarvis, A.P., Gruiz, K., 2012. Ecotoxicity of fluvial sediments downstream of the Ajka red mud spill, Hungary. *J. Environ. Monit.* 14, 2063–2071.
- Kobayashi, N., Okamura, H., 2005. Effects of heavy metals on sea urchin embryo development. Part 2. Interactive toxic effects of heavy metals in synthetic mine effluents. *Chemosphere* 61, 1198–1203.
- Kruse, N.A., Bowman, J., Lopez, D., Migliore, E., Jackson, G.P., 2014. Characterization and fate of polychlorinated biphenyls, polychlorinated dibenzo-p-dioxins and polychlorinated dibenzofurans in soils and sediments at the Portsmouth Gaseous Diffusion Plant, Ohio. *Chemosphere* 114, 93–100.
- Mišík, M., Burke, I.T., Reismüller, M., Pichler, C., Rainer, B., Mišíková, K., Mayes, W.M., Knasmueller, S., 2014. Red mud a byproduct of aluminum production contains soluble vanadium that causes genotoxic and cytotoxic effects in higher plants. *Sci. Total Environ.* 493, 883–890.
- Olszewska, J.P., Meharg, A.A., Heal, K.V., Carey, M., Gunn, I.D., Searle, K.R., Winfield, I.J., Spears, B.M., 2016. Assessing the legacy of red mud pollution in a shallow freshwater lake: arsenic accumulation and speciation in macrophytes. *Environ. Sci. Technol.* 50, 9044–9052.
- Pagano, G., Esposito, A., Bove, P., de Angelis, M., Rota, A., Giordano, G.G., 1983. The effects of hexavalent and trivalent chromium on fertilization and development in sea urchins. *Environ. Res.* 30, 442–452.
- Pagano, G., His, E., Beiras, R., De Biase, A., Korkina, L.G., Iaccarino, M., Oral, R., Quiniou, F., Warnau, M., Trieff, N.M., 1996. Cytogenetic, developmental and biochemical effects of aluminum, iron and their mixture in sea urchins and mussels. *Arch. Environ. Contam. Toxicol.* 31, 466–474.
- Pagano, G., Korkina, L.G., Iaccarino, M., De Biase, A., Deeva, I.B., Doronin, Y.K., Guida, M., Melluso, G., Meriç, S., Oral, R., Trieff, N.M., Warnau, M., 2001. Developmental, cytogenetic and biochemical effects of spiked or environmentally polluted sediments in sea urchin bioassays. In: Garrigues, P., Walker, C.H., Barth, H. (Eds.), *Biomarkers in Marine Ecosystems: A Practical Approach*. Elsevier, Amsterdam, pp. 85–129.
- Pagano, G., De Biase, A., Doronin, Y.K., Iaccarino, M., Meriç, S., Petruzzelli, D., Tünay, O., Warnau, M., Trieff, N.M., 2002a. Bauxite manufacturing residues from Gardanne (France) and Portovesme (Italy) exert different patterns of pollution and toxicity to sea urchin embryos. *Environ. Toxicol. Chem.* 21, 1272–1278.
- Pagano, G., Meriç, S., De Biase, A., Iaccarino, M., Petruzzelli, D., Tünay, M., Warnau, M., 2002b. Toxicity of bauxite manufacturing by-products in sea urchin embryos. *Ecotoxicol. Environ. Saf.* 51, 28–34.
- Pagano, G., Guida, M., Tommasi, F., Oral, R., 2015. Environmental effects and toxicity mechanisms of rare earth elements – knowledge gaps and research prospects. *Ecotoxicol. Environ. Saf.* 115C, 40–48.
- Pagano, G., Guida, M., Trifuoggi, M., Thomas, P.J., Palumbo, A., Romano, G., Oral, R., 2017. Sea urchin bioassays in toxicity testing: I. Inorganics, organics, complex mixtures and natural products. *Expert Opin. Environ. Biol.* 6, 1.
- Raja, R., Nayak, A.K., Shukla, A.K., Rao, K.S., Gautam, P., Lal, B., Tripathi, R., Shahid, M., Panda, B.B., Kumar, A., Bhattacharyya, P., Bardhan, G., Gupta, S., Patra, D.K., 2015. Impairment of soil health due to fly ash-fugitive dust deposition from coal-fired thermal power plants. *Environ. Monit. Assess.* 187, 679.
- Ren, J., Chen, J., Han, L., Wang, M., Yang, B., Du, P., Li, F., 2018. Spatial distribution of heavy metals, salinity and alkalinity in soils around bauxite residue disposal area. *Sci. Total Environ.* 628, 1200–1208.
- Ruwei, W., Jiamei, Z., Jingjing, L., Liu, G., 2013. Levels and patterns of polycyclic aromatic hydrocarbons in coal-fired power plant bottom ash and fly ash from Huainan, China. *Arch. Environ. Contam. Toxicol.* 65, 193–202.
- Sánchez-Marín, P., Beiras, R., 2012. Quantification of the increase in Pb bioavailability to marine organisms caused by different types of DOM from terrestrial and river origin. *Aquat. Toxicol.* 110–111, 45–53.
- Trieff, N.M., Romaña, L.A., Esposito, A., Oral, R., Quiniou, F., Iaccarino, M., Alcock, N., Ramaniyam, V.M.S., Pagano, G., 1995. Effluent from bauxite factory induces developmental and reproductive damage in sea urchins. *Arch. Environ. Contam. Toxicol.* 28, 173–177.
- Twardowska, I., Schramm, K.W., 2000. Occurrence of persistent organic pollutants (PAHs, PCDD and PCDF) in fly ash generated in coal-fired thermal and power plants in Silesia, Poland. *Cent. Eur. J. Public Health* 8 (Suppl.), 6–8.
- U.S. EPA, 2007. Method 3051A (SW-846): Microwave Assisted Acid Digestion of Sediments, Sludges, and Oils, Revision 1. Washington, DC.
- Vazquez, L.C., 2013. Unraveling a municipal effluent's toxicity to *Tripneustes gratilla* sperm fertilization. *Environ. Toxicol. Chem.* 32, 1382–1387.
- Wikström, E., Ryan, S., Touati, A., Gullet, B.K., 2003. Key parameters for de novo formation of polychlorinated dibenzo-p-dioxins and dibenzofurans. *Environ. Sci. Technol.* 37, 1962–1970.
- Willhite, C.C., Karyakina, N.A., Yokel, R.A., Yenugadhathi, N., Wisniewski, T.M., Arnold, I.M., Momoli, F., Krewski, D., 2014. Systematic review of potential health risks posed by pharmaceutical, occupational and consumer exposures to metallic and nanoscale aluminum, aluminum oxides, aluminum hydroxide and its soluble salts. *Crit. Rev. Toxicol.* 4 (44 Suppl.), S1–S80.
- Xu, G., Ding, X., Kuruppu, M., Zhou, W., Biswas, W., 2018. Research and application of non-traditional chemical stabilizers on bauxite residue (red sand) dust control, a review. *Sci. Total Environ.* 616–617, 1552–1565.
- Xue, S., Zhu, F., Kong, X., Wu, C., Huang, L., Huang, N., Hartley, W., 2016. A review of the characterization and revegetation of bauxite residues (Red mud). *Environ. Sci. Pollut. Res. Int.* 23, 1120–1132.